ResearchGate

See discussions, stats, and author profiles for this publication at: https://www.researchgate.net/publication/258080853

Plasma focus ion beam fluence and flux—For various gases

Article *in* Physics of Plasmas · June 2013

DOI: 10.1063/1.4811650

CITATIONS
26

READS
28

2 authors:

Sing Lee
INTI International University
393 PUBLICATIONS **3,547** CITATIONS
SEE PROFILE

Sor Heoh Saw
Nilai University, Negeri Sembilan, Malaysia
98 PUBLICATIONS **911** CITATIONS
SEE PROFILE

Available from: Sing Lee
Retrieved on: 06 October 2016

Plasma focus ion beam fluence and flux—For various gases

S. Lee and S. H. Saw

Citation: Phys. Plasmas **20**, 062702 (2013); doi: 10.1063/1.4811650
View online: http://dx.doi.org/10.1063/1.4811650
View Table of Contents: http://pop.aip.org/resource/1/PHPAEN/v20/i6
Published by the AIP Publishing LLC.

Additional information on Phys. Plasmas

Journal Homepage: http://pop.aip.org/
Journal Information: http://pop.aip.org/about/about_the_journal
Top downloads: http://pop.aip.org/features/most_downloaded
Information for Authors: http://pop.aip.org/authors

ADVERTISEMENT

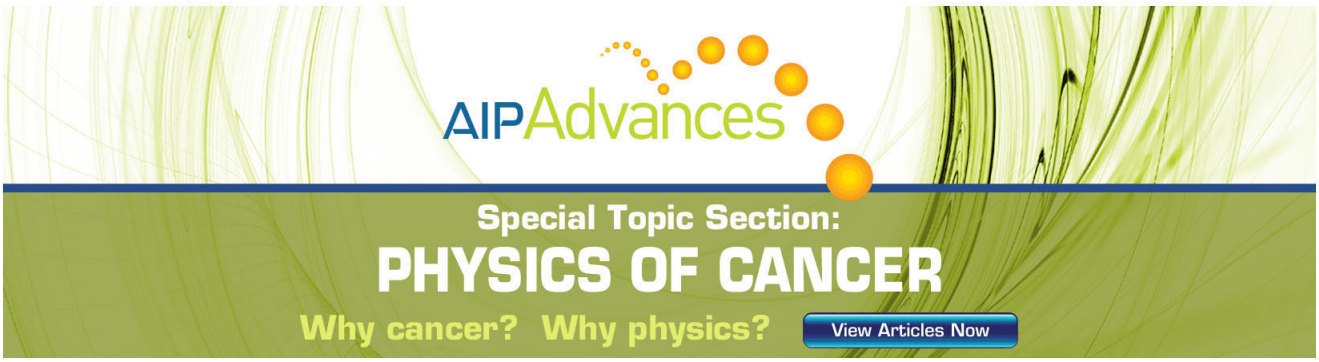

Plasma focus ion beam fluence and flux—For various gases

S. Lee[1,2,3] and S. H. Saw[1,2,a)]
[1]*Centre for Plasma Research, INTI International University, 71800 Nilai, Malaysia*
[2]*Institute for Plasma Focus Studies, 32 Oakpark Drive, Chadstone 3148, Australia*
[3]*Physics Department, University of Malaya, Malaysia*

(Received 21 April 2013; accepted 13 May 2013; published online 19 June 2013)

A recent paper derived benchmarks for deuteron beam fluence and flux in a plasma focus (PF) [S. Lee and S. H. Saw, Phys. Plasmas **19**, 112703 (2012)]. In the present work we start from first principles, derive the flux equation of the ion beam of any gas; link to the Lee Model code and hence compute the ion beam properties of the PF. The results show that, for a given PF, the fluence, flux, ion number and ion current decrease from the lightest to the heaviest gas except for trend-breaking higher values for Ar fluence and flux. The energy fluence, energy flux, power flow, and damage factors are relatively constant from H_2 to N_2 but increase for Ne, Ar, Kr and Xe due to radiative cooling and collapse effects. This paper provides much needed benchmark reference values and scaling trends for ion beams of a PF operated in any gas. © *2013 AIP Publishing LLC*.
[http://dx.doi.org/10.1063/1.4811650]

I. INTRODUCTION

A recent survey[1] of ion beam measurements in plasma focus (PF) devices showed a wide range of experimental methods producing results (using mostly inappropriate, even confusing units) which are neither correlated among the various methods and machines nor show any discernible scaling or trend. That paper suggested that since the ion beam exits the focus pinch as a narrow beam with little divergence, the exit beam is best characterized by the yield of ion number m^{-2} per shot which the paper termed the fluence per shot. Defining the fluence as the basic PF property for ion yield led naturally to defining other properties including the flux (fluence s^{-1}), the energy fluence and the energy flux, number of ions per shot, and beam ion current. In order to compute the fluence, the paper noted that D-D neutron yield and scaling were already successfully computed by means of a beam-gas target neutron generating mechanism in the Lee Model code. This suggested that the deuteron fluence was already implicit in the neutron yield equation. It was hence a natural step to deduce the deuteron fluence equation, incorporate it in the Lee Model code, and hence compute the fluence and other ion beam properties. This was done for a number of machines. The main results[1] were that: deuteron number fluence (ions m^{-2}) and energy fluence (J m^{-2}) computed as $2.4–7.8 \times 10^{20}$ and $2.2–33 \times 10^{6}$, respectively, were independent of E_0 from 0.4 to 486 kJ. Typical PF devices with inductance in the range 33–55 nH produce $1.2–2 \times 10^{15}$ ions per kJ carrying 1.3%–4% E_0 at mean ion energy 50–200 keV. Thus that paper defined appropriate ion properties and established reference numbers for these properties for the case of deuterons. Additionally, information on ion beam damage factor and the post-focus pinch fast plasma stream (FPS) was also obtained.

A natural next question is: What are the corresponding reference numbers for ions produced in PF devices operated in other gases? This question is not only of basic importance to provide reference numbers for measurements but may also help in the selection of gases for materials application such as damage studies where gases with high ion beam damage factor and power flow may be important or in materials fabrication where uniformity may require a gas having a lower damage factor whilst having higher values of fast plasma stream energy with a bigger radial distribution.

The PF dynamics may be divided into two major phases: the axial and the radial. In the axial phase, a current sheath is driven down the coaxial channel between the anode and the concentric cylindrical cathode in the direction from left to right in Fig. 1. At the end of the axial phase, the radial phase begins in which a cylindrical current sheath is driven radially inwards preceded by a shock wave.[2] When the shock wave goes on-axis, a stagnated pinch column is formed with the boundary of the stagnated region moving outwards. This boundary may be characterised as a reflected shock wave moving radially outwards, separating a stagnated column of doubly shocked gas of higher density and temperature from the outer region of inward streaming plasma which is driven by the radially inward moving radial current sheath (piston). When the outwardly moving reflected shock meets the incoming piston the focus pinch phase begins, in which the pinch boundary moves slowly either inwards or outwards depending on the relative strengths of the magnetic pressure exerted by the piston and the increased hydrostatic pressure of the stagnated pinch. The radiation from the dense hot pinch plasma may become sufficient to affect the plasma dynamics in terms of radiative cooling and radiative collapse[3] in the case of high Z gases such as Ar, Kr or Xe or even Ne. From experimental observations, it has been suggested[4] that Ar ($Z = 18$) is the transition gas in the sense that for gases with $Z < 18$ the pinching and any radiative collapse proceed as a column whereas for gases with $Z > 18$ radiative collapse breaks the column up into a line of collapsed dense hot spots. We return to this point later in the paper when it becomes pertinent to our results. The dynamics of the current sheath

a)E-mail: sorheoh.saw@newinti.edu.my

 © 2013 AIP Publishing LLC

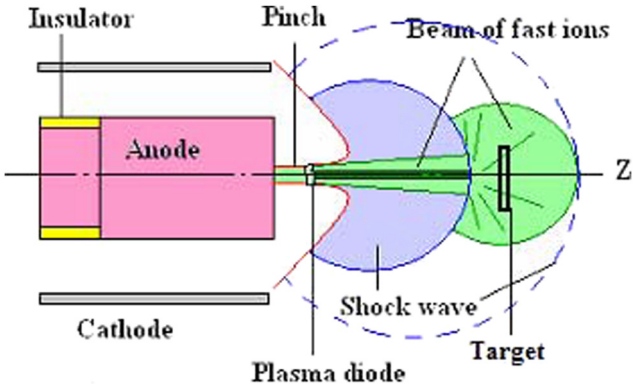

FIG. 1. Schematic of the post-pinch FIB(fast ion beam) and FPS represented here by a shock wave. Reprinted with permission from Pimenov *et al.*, International Atomic Energy Agency, Nuclear Research Applications and Utilization of Accelerators, Proceedings of an International Topical Meeting held in Vienna, Austria, 4–8 May 2009, IAEA, Vienna, (2010).

causes large temporal changes of inductance dL/dt and consequential rate of change of currents dI/dt. Large electric fields are induced. These and the extreme conditions of the pinch lead to observed plasma disruptions. Besides electromagnetic radiations from the focus, particles are also emitted. Generally, ion beams are emitted in the axial direction away from the anode and relativistic electrons (REB) towards the anode.

In this paper, we focus on the ion beams. We use the mechanism proposed by Gribkov *et al.*[5] A beam of fast ions is produced by diode action in a thin layer close to the anode (see Fig. 1),[6] with plasma disruptions in the pinch generating the necessary high voltages. These disruptions also terminate the quasi-static nature of the pinch so that the duration of the pinch[7] may be related to the transit time of relevant small disturbances across the pinch column.

During the radial compression phase, energy is imparted to the plasma and stored in the increasing inductance of the pinch column. Some of this accumulating energy is emitted as radiation, primarily line radiation in the case of high Z gases, and also provided to the ion and REB. The remnant energy may be considered to manifest in the FPS.

II. THE METHOD

A. The ion beam flux and fluence equations

We now proceed to estimate the flux of the ion beam.

We write the ion beam flux as

$$J_b = n_b v_b,$$

where n_b = number of beam ions N_b divided by volume of plasma traversed by the beam; and v_b is the effective speed of the beam ions. All quantities are expressed in SI units, except where otherwise stated. Note that $n_b v_b$ has units of ions per $m^{-2}\,s^{-1}$.

We then proceed to derive n_b from the kinetic energy of the beam ions (BKE) and pinch inductive energy (PIE) considerations.

The BKE is contributed from the total number of beam ions N_b where each beam ion has a mass Mm_p and speed v_b and is represented by $BKE = (1/2)N_b Mm_p v_b^2$. The mass of the proton m_p is 1.673×10^{-27} kg and M is the mass number of ion, e.g., neon ion has mass number M = 20.

This BKE is imparted by a fraction f_e of the PIE represented by $PIE = (1/2)L_p I_{pinch}^2$ where $L_p = (\mu/2\pi)\,(\ln[b/r_p])z_p$ is the inductance of the focus pinch; $\mu = 4\pi \times 10^{-7}$ H m^{-1}; b is the outer electrode of the plasma focus carrying the return current; r_p is the pinch radius carrying the current through the plasma; z_p is the length of the pinch; and I_{pinch} is the pinch current value taken at start of pinch. Thus

$$(1/2)N_b Mm_p v_b^2 = f_e(1/2)(\mu/2\pi)(\ln[b/r_p])\, z_p I_{pinch}^2.$$

This gives

$$\begin{aligned} n_b &= N_b/(\pi r_p^2 z_p) \\ &= (\mu/[2\pi^2 m_p])(f_e/M)\{(\ln[b/r_p])/(r_p^2)\}(I_{pinch}^2/v_b^2). \end{aligned} \quad (1)$$

Next, we proceed to derive v_b from the accelerating voltage provided by the diode voltage U to an ion. Each ion with effective charge Z_{eff} is given kinetic energy of (1/2) $Mm_p v_b^2$ by diode voltage U. Thus

$$(1/2)Mm_p v_b^2 = Z_{eff} eU,$$

where e is the electronic (or unit) charge 1.6×10^{-19} C.

Hence

$$v_b = (2e/m_p)^{1/2}(Z_{eff}/M)^{1/2}U^{1/2}. \quad (2)$$

Now, we take Eq. (1) and combine with Eq. (2), and noting that $(\mu/[2.83\pi^2(em_p)^{1/2}]) = 2.75 \times 10^{15}$, we have the flux equation as follows:

$$\begin{aligned} \text{Flux (ions m}^{-2}\text{s}^{-1}) = J_b &= 2.75 \times 10^{15}\,(f_e/[M Z_{eff}]^{1/2}) \\ &\times \{(\ln[b/r_p])/(r_p^2)\}(I_{pinch}^2)/U^{1/2}. \end{aligned} \quad (3)$$

The fluence is the flux multiplied by pulse duration τ. Thus

$$\begin{aligned} \text{Fluence (ions m}^{-2}) &= 2.75 \times 10^{15}\tau\,(f_e/[M Z_{eff}]^{1/2}) \\ &\times \{(\ln[b/r_p])/(r_p^2)\}(I_{pinch}^2)/U^{1/2}. \end{aligned} \quad (4)$$

We now compare Eq. (4) for fluence per shot with the equation for fluence derived for deuterons by Lee and Saw.[1] In that paper, the pulse duration is taken as the pinch duration and hence is taken as proportional to anode radius which also has a proportional relationship to pinch length[7] z_p. We may take pinch duration as 10 ns per mm pinch radius and pinch length is about 1 cm per mm pinch radius.[7] Hence, pinch duration is 1 μs per m pinch length, giving us the approximate relationship: $\tau = 10^{-6} z_p$. We then have

$$\begin{aligned} \text{Fluence (ions m}^{-2}) &= 2.75 \times 10^{9}\pi z_p(f_e/[M Z_{eff}]^{1/2}) \\ &\times \{(\ln[b/r_p])/(\pi r_p^2)\}(I_{pinch}^2)/U^{1/2}. \end{aligned}$$

For deuteron where M = 2 and $Z_{eff} = 1$; and if we take $f_e = 0.14$ (i.e., 14% of PIE is converted into BKE) then we have

$$\text{Fluence (ions m}^{-2}) = J_b\tau = 8.5 \times 10^8 I_{pinch}{}^2 z_p \times \{(\ln[b/r_p])/(\pi r_p{}^2 U^{1/2})\}. \quad (5)$$

Equation (5) is exactly the same as Eq. (3) of the paper by Lee and Saw[1] used to determine the deuteron ion beam fluence and flux.

In other words starting from first principles, we have derived exactly the same equation as Lee and Saw[1] did using empirical formula derived with quantities all with proportional constants finally calibrated at a 0.5 MJ point of neutron yield. In this present derivation from first principles, we need only one additional condition $f_e = 0.14$ (the fraction of energy converted from PIE into BKE) and the approximate scaling $\tau = 10^{-6} z_p$. This additional condition of $f_e = 0.14$ is equivalent to ion beam energy of 3%–6% E_0 for cases when the PIE holds 20%–40% of E_0 as observed for type 1 or low inductance PF.[8] We also conclude that the flux equation (3) derived here is the more basic equation to use as it does not have to make any assumptions about the ion beam pulse duration.

According to Eqs. (3) and (4) the flux and fluence are dependent on $(MZ_{eff})^{-1/2}$, if all other pinch properties remain equal. From this simple dependence one would expect the flux and fluence to reduce as we progress from H_2 to D_2, He to Kr and Xe. However, the pinch properties, primarily the pinch radius do change drastically for different gases at different regimes of operation; due to thermodynamic and radiative effects. The change in r_p and associated and consequential changes in pinch dynamics and other properties, as computed from the code we use in this paper, have profound effects on modifying this simple dependence.

We summarise the assumptions:

1. Ion beam flux J_b is $n_b v_b$ with units of ions m^{-2} s^{-1}.
2. Ion beam is produced by diode mechanism.[5]
3. The beam is produced uniformly across the whole cross-section of the pinch.
4. The beam speed is characterized by an average value v_b.
5. The BKE is a fraction f_e of the PIE, taken as 0.14 in the first instance; to be adjusted as numerical experiments indicate.
6. The beam ion energy is derived from the diode voltage U.
7. The diode voltage U is $U = 3V_{max}$ taken from data fitting in extensive earlier numerical experiments,[2,9,10] where V_{max} is the maximum induced voltage of the pre-pinch radial phase. However for cases exhibiting strong radiative collapse, the strong radiative collapse generates an additional induced voltage Vmax*. This voltage is very large and from extensive numerical experiments appears to be a reasonable estimate of the beam ion energy from the point of view of the various energy distributions including the ion beam energy relative to the fast plasma stream energy. Hence, the feedback from our extensive examinations of the data suggests that we take, in such cases, U = Vmax*.

The value of the ion flux is deduced in each situation for specific machine using specific gas by computing the values of Z_{eff}, r_p, I_{pinch}, and U by configuring the Lee Model code with the parameters of the specific machine and specific gas. The code and the procedure are discussed in more detail in a later section.

B. Consequential properties of the ion beam

Once the flux is determined, the following quantities are also computed:

(a) Energy flux or power density flow (W m^{-2}) is computed from $\mathbf{J_b} \times Z_{eff}U$ noting the need to multiply by 1.602×10^{-19} to convert eV to J.
(b) Power flow (W) is computed from energy flux × pinch cross-section.
(c) Current density (A m^{-2}) is computed from $\mathbf{J_b}$ × ion charge eZ_{eff}.
(d) Current (A) is computed from Current density × pinch cross-section.
(e) Ions per seconds (ions s^{-1}) are computed from $\mathbf{J_b}$ × pinch cross-section.
(f) Fluence (ions m^{-2}) is computed from $\mathbf{J_b} \times \tau$.
(g) Energy fluence (J m^{-2}) is computed from $\mathbf{J_b} \times \tau \times Z_{eff}U$.
(h) Number of ions in beam (ions) is computed from Fluence × pinch cross-section.
(i) Energy in beam (J) is computed from Number of ions in beam × $Z_{eff}U$.
(j) Damage Factor (W m^{-2} $s^{0.5}$) is computed from $\mathbf{J_b} \times Z_{eff}U \times \tau^{1/2}$.
(k) Energy of fast plasma stream (J).

Experimentally it is found that as the focus pinch starts to break up a fast shock wave exits the plasma focus pinch in the axial direction preceding the ion beams which rapidly catches up and overtakes it.[5,6] Associated with this fast post-pinch axial shock wave is a FPS. We estimate the energy of the FPS by computing the work done by the magnetic piston through the whole radial phase from which is subtracted twice the ion beam energy (the second count being for the oppositely directed relativistic electron beam which we assume to have the same energy as the ion beam) and from which is further subtracted the radiation yield[2,11–15] of the plasma pinch.

C. The Lee model code

The code[2] couples the electrical circuit with PF dynamics, thermodynamics, and radiation. It is energy-, charge-, and mass- consistent. It was described in 1983 (Ref. 16) and used in the design and interpretation of experiments.[17–19] An improved 5-phase code[2] incorporating finite small disturbance speed,[20] radiation and radiation-coupled dynamics was used,[21–23] and was web-published[24] in 2000. Plasma self-absorption was included[24] in 2007. It has been used extensively as a complementary facility in several machines, for example, UNU/ICTP PFF,[17,19,21–23] NX2,[23,25] NX1,[23] DENA.[26] It has also been used in other machines for design and interpretation including sub-kJ PF machines,[27] FNII,[28] and the UBA hard x-ray source.[29] Information computed includes axial and radial dynamics,[17,18,21,23,30] SXR emission characteristics and yield,[11–15,22,23,25,31] design of

machines,[16,17,21–23] optimization of machines,[2,11,17,24] and adaptation to Filippov-type DENA.[26] Speed-enhanced PF[21] was facilitated. Plasma focus neutron yield calculations,[10,32] current and neutron yield limitations,[9,11] deterioration of neutron scaling (neutron saturation),[33,34] radiative collapse,[3] current-stepped PF[35] and extraction of diagnostic data,[36–38] and anomalous resistance data[8,39] from current signals have been studied using the code.[2] As already pointed out in the introduction, the Model code has recently been used to produce reference numbers for deuteron beam number and energy fluence and flux and scaling trends for these with PF storage energy.[1] The present paper extends the beam ion calculations to include all gases.

D. Procedure used in the numerical experiments

We use the NX2 (Refs. 2, 23, and 25) for these numerical experiments to study the number and energy flux and fluence in various gases including hydrogen, deuterium, helium, nitrogen, neon, argon, krypton, and xenon. This gives us a good range of data in terms of mass and charge numbers. We configure the NX2 as follows:[2,23]

Capacitor bank parameters: $L_0 = 20$ nH; $C_0 = 28\ \mu$F, $r_0 = 2.3\ m\Omega$.

Tube parameters: $b = 4.1$ cm; $a = 1.9$ cm, $z_0 = 5$ cm.

Operating parameters: $V_0 = 14$ kV; $P_0 =$ appropriate range of pressures in each gas.

Model parameters: $f_m = 0.06$, $f_c = 0.7$, $f_{mr} = 0.16$, and $f_{cr} = 0.7$

The parameters are: L_0 is the static inductance[37] defined as inductance of discharge circuit without any plasma dynamics (for example, with the bank short-circuited at the input to the plasma focus tube), C_0 is the bank capacitance, r_0 is the short circuited resistance of the discharge circuit, b is the cathode radius, a is the anode radius, z_0 is the effective anode length, V_0 is the bank charging voltage, and P_0 is the operating pressure. A range of pressures is chosen so that the PF axial run-down time encompasses at least from 0.5 to 1.3 of the short-circuit rise time which is approximately $1.57 \times (L_0C_0)^{0.5}$. Within this range lies the optimum (matched) pressure with the strongest energy transfer into the PF pinch. We also want to reach high enough pressures so that the focus pinch is almost not occuring as defined by the condition that the reflected shock is barely able to reach the rapidly decelerating magnetic piston. The model parameters f_m, f_{mr} and f_c, f_{cr} are mass and current factors[2,15,18,40–42] of axial and radial phases; and take into account all mechanisms in the plasma focus which cause the mass distributions and current distributions to deviate away from the ideal situation.[2] These parameters are obtained from fitting the computed current traces to the measured current traces whilst varying the parameters.[2,11–14]

For each shot, the dynamics is computed and displayed by the code[2] which also calculates and displays the ion beam properties listed in Sec. II B above. For H_2, D_2, He, N_2 and Ne, the procedure is relatively simple even though Ne already exhibits enhanced compression due to radiative cooling.

For Ar, Kr and Xe, the radiation yield (almost wholly the line yield which is proportional to Z^4, where Z is the atomic number) is so severe that the radiative collapse has to be adjusted by limiting the minimum radius of compression r_{min} (defined by the radius ratio r_{min}/a) and time of the pinch in order that the remnant FPS energy remains at least minimally positive. This adjustment involves studying the line yield, the ion beam energy and the FPS energy as well as the value of f_e point by point. The final results contain a degree of uncertainty in the sense that each strong radiative collapse point could be adjusted a little differently (by 10% or so) in distribution of energies. However, extensive series of runs show that despite the uncertainty of the few strongest radiative collapse points for each gas the total picture of energy distributions with pressure is clear and unambiguous. This will be discussed in Sec. III.

We need to point out here that we model the pinch radiative collapse with the collapse of the pinch as a whole column whereas experimental observations[4] indicate that Ar is the transition gas below which (lighter gases) the pinch compresses as a column whilst for heavier gases (Kr and Xe) the compression breaks up into a line of hot spots. Our numerical experiments indicate from energy considerations that when the compression breaks up into a line of hot spots the electric current does not all flow through the hot spots but there is a substantial flow of current in a far less compressed column in which the line of hot spots is "embedded," so that the total effect in terms of energy transfer and inductance is less severe than indicated by our collapse-as-a-column modelling. That is the reason why our FPS energy goes negative which serves as an indicator for us to adjust pinch radius and time until the FPS reaches a reasonable positive value.

III. RESULTS AND DISCUSSIONS

A. Discharge current and general dynamics

Figure 2(a) shows the discharge current rising from zero to almost 400 kA in just over 1 μs. For good energy coupling into the pinch, the radial phase should start around this time.[2] For NX2 operated in D_2 at 15 Torr the matching is good as seen in Fig. 1(a) where the radial phase is indicated by the current rolling over into the dip lasting from just after 1 μs to 1.2 μs. The computed radial trajectories comprising the shock front the reflected shock and the magnetic piston are shown in Fig. 2(b).

For comparison, Fig. 3(a) shows the discharge current for Ar at 2 Torr. Note the more severe dip (an additional almost vertical dip following the initial more gentle dip) and that the tube voltage has a second spike that rises to more than 150 kV. The corresponding radial trajectories are shown in Fig. 3(b) where it is seen that the Ar shock-piston separation is much thinner than that of the D_2 radial phase. This is due to the Ar ions being highly but not fully ionised and the reduction of its specific heat ratio[43] to below the perfect gas limit of 5/3. Note also that the piston collapses to very small radius during the pinch. That radiative collapse is caused by the intense radiation of Ar which reduces its hydrostatic pressure thus allowing the magnetic pressure to compress the column much more severely than the case of D_2.

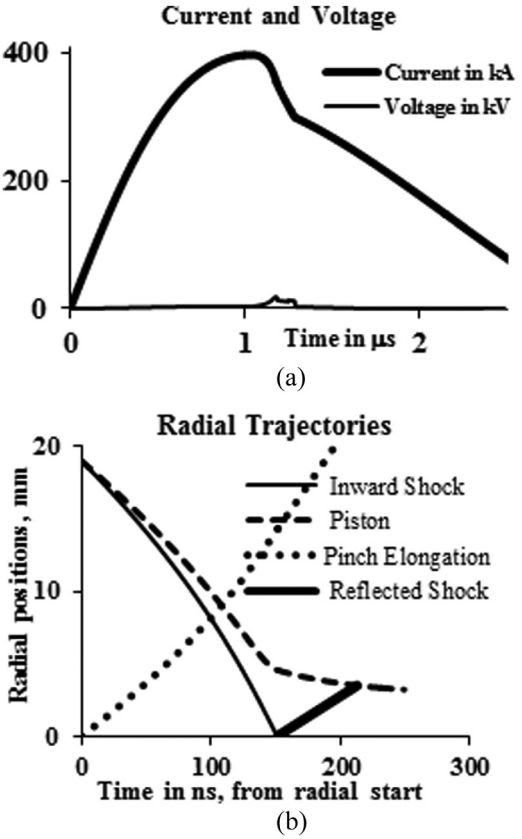

FIG. 2. (a) NX2 in 15 Torr D_2—Circuit current and tube voltage. (b) NX2 in 15 Torr D_2—Radial trajectories of inward shock and reflected shock, inward piston. The dotted line represents the axial elongation of the imploding column.

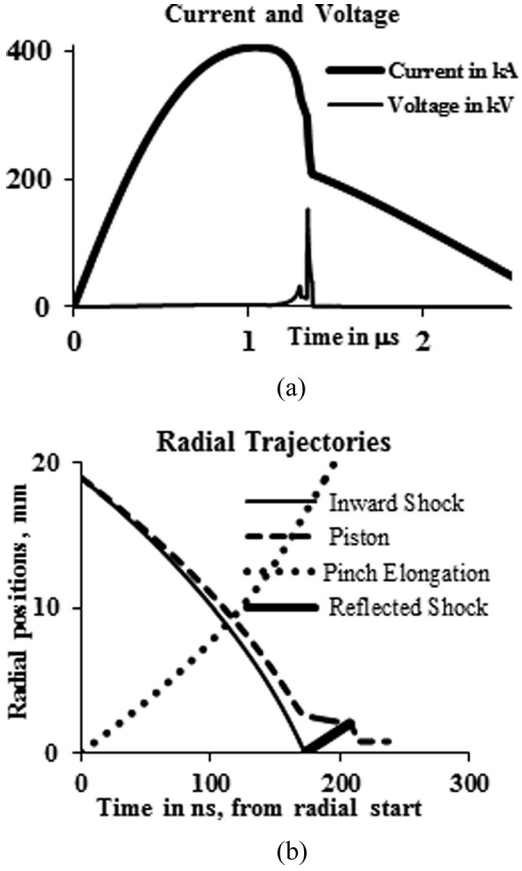

FIG. 3. (a)NX2 in 2 Torr Ar—Circuit current and tube voltage. (b) NX2 in 2 Torr Ar—Radial trajectories of inward shock and reflected shock, inward piston. The dotted line represents the axial elongation of imploding column.

B. Radius ratios for various gases

Using H_2, we run experiments from 1 Torr up until best energy matching at 30 Torr and then beyond as the pinch becomes weaker. For D_2 and He, good matching is around 15 Torr (as shown in Fig. 2(a) for D_2); for N_2, it is at 2 Torr. We found good matching for Ne, Ar, Kr, and Xe at 4 Torr, 2 Torr, 1 Torr and 0.5 Torr, respectively. Figure 4 illustrates the different compression of the plasma focus pinch for different gases. In H_2, D_2 and He at low pressures, the radius ratio is about 0.15, the 3 graphs staying together up to 10 Torr. Above 10 Torr (not shown in the figure), the radius ratio of D_2 and He separate from that of H_2 being slightly higher; all 3 graphs rising steadily to 0.2 at the highest operational focus pressures. For N_2, the radius ratio drops from 0.15 at to a value about 0.13. This is due to thermodynamic specific heat ratio (SHR) effects.[43] At low pressures, the shocks waves are faster and the temperature high enough so that the pinch is fully ionised with a SHR of practically 5/3. At higher pressures around 1 Torr, the N2 pinch is no longer fully ionised and its SHR drops significantly below 5/3 increasing its compressibility,[43] thus the lower pinch radius ratio of 0.13. Ne shows signs of radiatively enhanced compressions between 3 and 5 Torr indicated by the smaller radius ratio down to a minimum of 0.08 at 4 Torr. Argon shows strong radiative collapse with a radius ratio of 0.04 (a cut-off value used together with a pinch duration adjusted to be energy consistent; the procedure is discussed above Sec. II D) over a narrow range of pressure around 2.0 Torr. Krypton is strongly radiatively collapsed from 0.5 to 2 Torr and Xe over 0.3–1.5 Torr; these pressure ranges being a large proportion of their range of strong focus operation.

C. Ion beam flux for various gases

Figure 5 shows the flux in ions m^{-2} s^{-1} for the various gases. The H_2 curve has a value of 6×10^{27} at 1 Torr and rises steadily to a peak of 19×10^{27} at 25 Torr (outside the

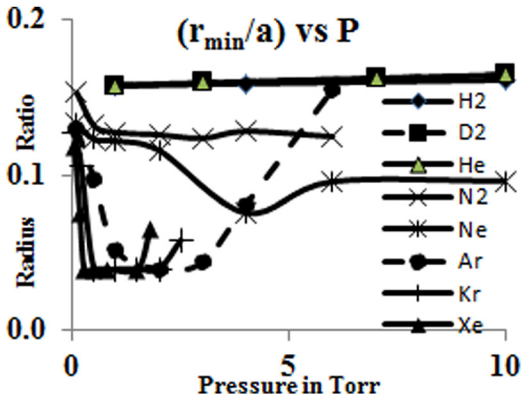

FIG. 4. Radius ratio vs P for different gases.

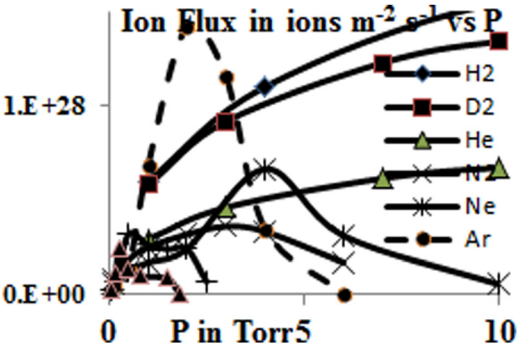

FIG. 5. Flux vs pressure for various gases.

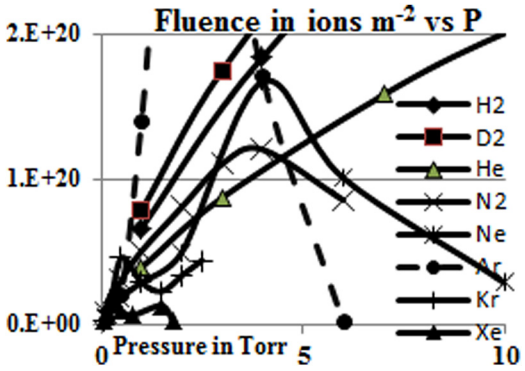

FIG. 6. Fluence vs pressure for various gases.

pressure range of the figure). The flux then drops gradually. The D_2 and He curve show the same trend with lower peak flux values of 14×10^{27} and 7×10^{27}, respectively, at 15 Torr. Nitrogen shows the same trend peaking at 3.6×10^{27} at 3 Torr. Neon shows an accentuated peak of 6.6×10^{27} appearing at 4 Torr corresponding to the observed radiatively collapsed compression at 4 Torr (see Fig. 4). Argon beam ion flux is even more obvious in displaying the effect of radiative collapse peaking at a highly accentuated 14×10^{27} at 2 Torr. For Kr although the radiative compression is even greater than Ar, the flux is fairly flat at 3×10^{27} in the pressure range of good energy transfer into the pinch in the region of 1 Torr. The accentuating effect on the flux (due to smaller radius ratio) is more than compensated by the opposing effect of much greater energy per ion. These two competing effects result in reduced ion numbers (see Fig. 7 discussed in Sec. III E). These competing effects (of reduced pinch radius and the reduced ion numbers) on the flux are more complicated than our first discussion here and will become clearer as we discuss the other properties. Xenon shows the same flat flux curve as Kr with a flat central value around 9×10^{26}. Thus we observe that the beam ion flux drops as the mass number of the ions increases, with accentuating factors provided by radiation-enhanced compression.

D. Ion beam fluence for various gases

Figure 6 shows the fluence in ions m^{-2} for the various gases. The shape of the curves and the trend with gases are very similar to the flux discussed in Sec. III C, the fluence being the flux multiplied by the estimated duration of the ion beam pulse duration. The peak values of the fluence (ions m^{-2}) range from 8×10^{20} for H_2 to 0.2×10^{20} for Xe; again with clearly enhanced values of 4.3×10^{20} and 1.7×10^{20} for Ar and Ne, respectively, due to radiative collapse. The values for each gas are placed in Table I for comparison of the ion beam properties.

TABLE I. NX2 Ion beam characteristics in a number of gases.

NX2	H_2	D_2	He	N_2	Ne	Ar	Kr	Xe
Pressure (Torr)	30	15	15	2	4	2	1 ((1)(1)	0.5
I_{peak} (kA)	397	397	397	395	406	406	408	400
I_{pinch} (kA)	222	222	222	215	208	209	210	213
z_p (cm)	2.8	2.8	2.8	2.8	2.8	3.4	2.5	2.4
r_p (cm)	0.33	0.32	0.32	0.24	0.14	0.08	0.08	0.08
τ (ns)	36.5	36.5	36.5	25.6	25.2	30	11.2	7.4
V_{max} (kV)/Vmax*	18.1	18.1	18.1	29	34	152*	1784*	4693*
Z_{eff}	1	1	2	6.4	8	11	13.5	13.6
Ion fluence ($\times 10^{20}$ m^{-2})	**7.0**	**5.2**	**2.6**	**0.8**	**1.7**	**4.3**	**0.29**	**0.1**
Ion flux ($\times 10^{27}$ m^{-2} s^{-1})	19	14	7	3.2	6.6	14	2.6	1.3
Mean ion energy (keV)	54	54	108	553	815	16740	24038	636294
En fluence ($\times 10^6$J m^{-2})	6.1	4.5	4.5	7.2	22	110	110	100
En flux ($\times 10^{13}$ W m^{-2})	17	12	12	28	87	380	1000	1300
Ion number/kJ ($\times 10^{14}$)	86	61	31	5.3	4	2.8	0.19	0.06
FIB energy (J)	205	146	146	130	143	207	204	179
FIB energy (%E_0)	7.5	5.3	5.3	4.7	5.2	7.5	7.4	6.5
IB current (kA)	103	74	74	58	56	45	10	5
Beam power ($\times 10^9$ kW)	**5.6**	**4**	**4**	**5.1**	**5.7**	**6.9**	**18**	**24**
DamFr ($\times 10^{10}$ W m^{-2} $s^{0.5}$)	**3.2**	**2.3**	**2.3**	**4.5**	**14**	**66**	**110**	**120**
Ion speed (cm/μs)	321	227	227	275	279	283	739	960
FPS En (J)	221	341	341	394	406	215	94	114
FPS En (%E_0)	8	12.4	12.4	14.3	14.8	7.8	3.4	4.1
FPS speed (cm/μs)	15.8	16.1	16	21	26.5	38	22	14

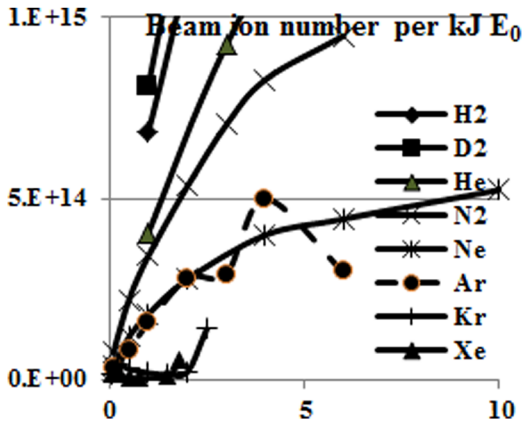

FIG. 7. Beam ion number per kJ as a function of pressure for various gases.

E. Beam ion number per kJ

The numerical experiments show that the beam ion number per kJ range from about 10^{16} (outside the pressure range of Fig. 7) for the lightest gases to 6×10^{12} for Xe in the radiative collapse regime. Argon reaches a peak numer per kJ of 5×10^{14}.

F. Beam current

The ion currents ranges from 108 kA for H_2 at 25 Torr (about 1/4 of the circuit I_{peak}) to 4 kA (1% of I_{peak}) for strongly compressed Xe at 1 Torr. The graphs show that the ion current drops with heavier gases and that radiative-collapse further reduces the ion current.

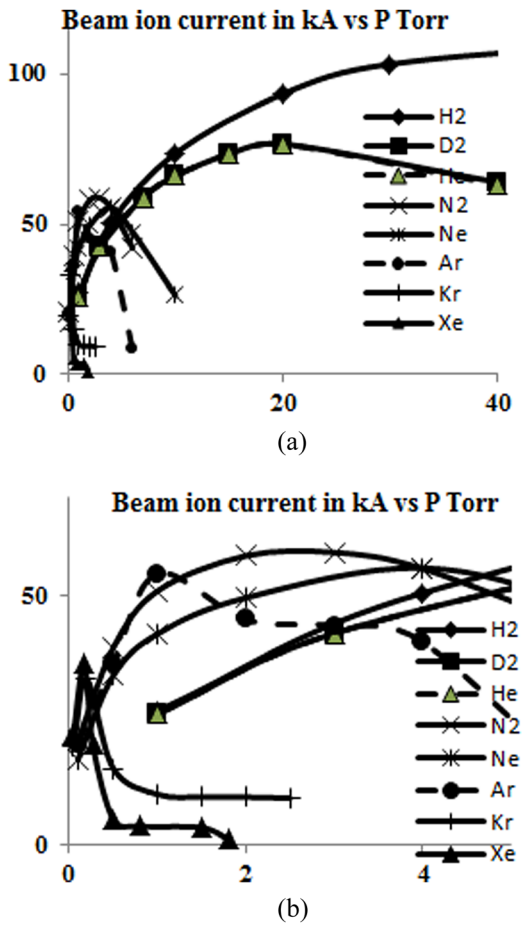

FIG. 8. (a) Beam ion current for various gases. (b) Ion currents (pressure expanded scale) to show the heavier gases.

G. Beam energy in the various gases

The results of the numerical experiments show that although the beam ion number and ion current are the lowest (see Figs. 7 and 8) for the heaviest gases Ar, Kr and Xe, yet these beams also carry similar amounts of energy at 7%–8% E_0 compared to 5%–8% for the other gases. This is because the greater energy per ion compensates for the low numbers of ions (Fig. 9).

H. Power flow

In terms of ion beam power flow, the 3 heaviest gases produce 7–24 $\times$ 10^9 W whereas the lightest gases only carry 4– 6 $\times$ 10^9 W (Fig. 10). This is due to the shorter pulse duration of the radiation-collapsed heavier gas pinches.

I. Damage factor

The damage factor defined as power flow density multiplied by (pulse duration)$^{0.5}$ reaches almost 110 $\times$ 10^{10} for Xe and is only 2 $\times$ 10^{10} for H_2. Argon has an intermediate damage factor of 66 $\times$ 10^{10}. The large values for Ar, Kr, and

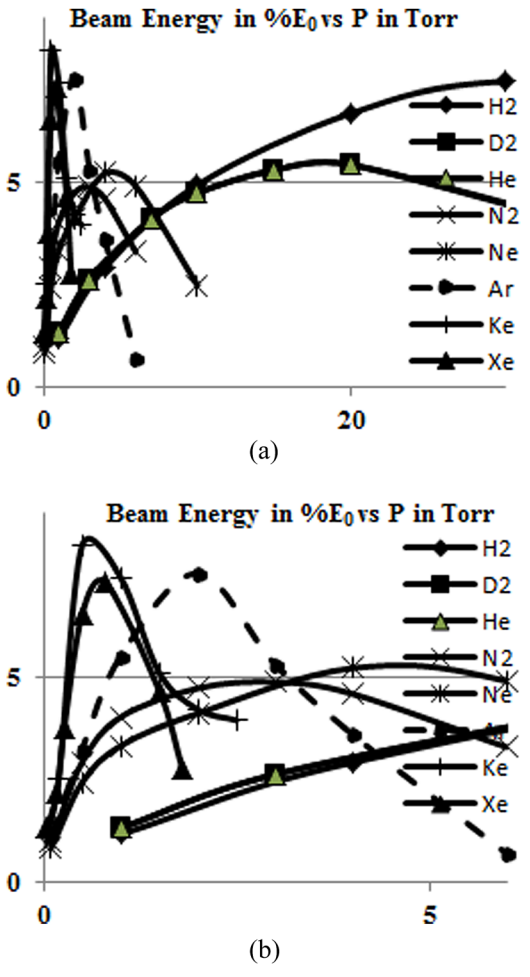

FIG. 9. (a) Beam energy as % E_0 in the various gases and (b) beam energy expanded in pressure scale.

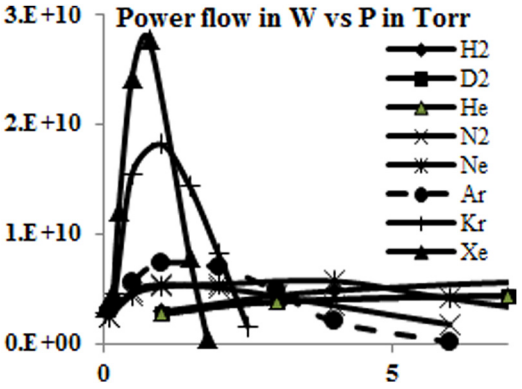

FIG. 10. Power flow for the various gases.

Xe are due to the very small radius ratios of the pinch columns due to radiative collapse (Fig. 11).

J. Energy of fast plasma stream

The FPS energy versus pressure curve has a simple shape for the lighter gases including H_2, D_2, He, N_2, and Ne, rising from a few % of E_0 towards a peak value of 13% E_0 (for the case of D_2; not shown in graph) and maintaining to

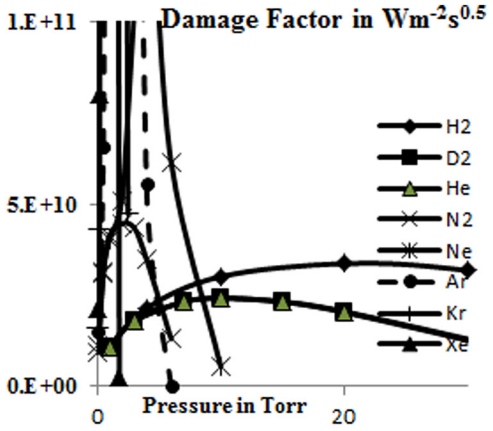

(a)

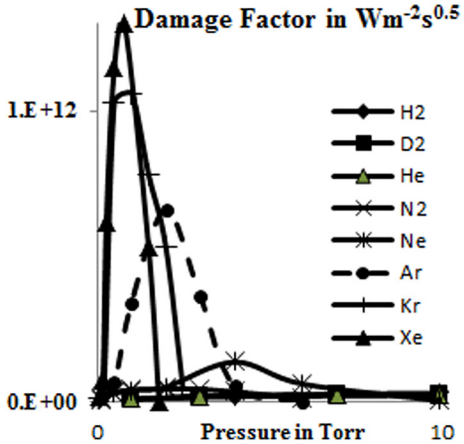

(b)

FIG. 11. (a) Damage factor showing the lighter gases (Ne, Ar, Kr, and Xe peaks out of scale). (b) Showing the heavier gases (lighter gases have too small damage factors to be seen on this scale).

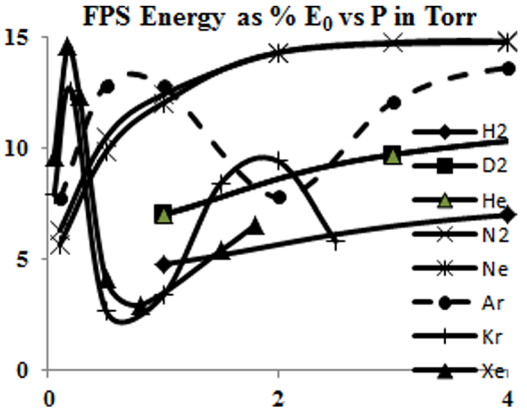

FIG. 12. Energy of FPS.

the highest operational pressures (Fig. 12). For Ne, a peak is observed at almost 15% at 4 Torr. Beyond this point, the combination of still large beam energies and also Ne line radiation depletes the already decreased pinch energy, thus reducing the remnant energy for the FPS. For the 3 heaviest gases, the situation is more complicated being compounded by the dynamics and energetics of the radiative collapse. For example, at low pressures the argon radial phase occurs before peak current, limiting the pinch energy and hence the FPS energy. As the pressure rises the pinch occurs at increasingly higher current, thus generating more pinch energy and also more FPS energy which reaches a peak value of 13% E_0 at 0.5 Torr. Beyond this pressure although energy matching continues to improve with the radial phase occuring at higher and higher currents, at least up to 2 Torr, the Ar line radiation is already large enough to cause strong radiative cooling. The radiative collapse generates large induced voltages enhancing the beam ion energy. Both these effects counter the rising pinch energy sufficiently to reduce the energy feeding the FPS to as low as 8% E_0 at 2 Torr. Beyond this pressure, the Ar line radiation gradually reduces; radiative cooling reduces and ion beam energy also drops. These effects are sufficient to counter the gradually reducing pinch energy due to the pinch occuring at reducing currents. The nett effect is that the FPS energy starts to rise and indeed continues to rise throughout the rest of the higher pressure operational regime for Ar. The energetics governing Kr and Xe is basically similar to the situation in Ar as is evidenced by similar FPS energy variation with pressure.

K. Tabulation of ion beam properties in various gases for comparison

The above results are tabulated for a comparative study as shown in Table I.

IV. CONCLUSION

In this paper, we deduce from first principles the flux equation of ion beams in PF for any gas. We then configure the Lee Model code as the NX2 using best estimated model mass and current factors obtained from fitting the computed current traces of several gases with experimentally measured current traces. The flux equation is incorporated into the

code and the number and energy flux and fluence from different gases are computed together with other relevant properties.

The results portray the properties of the ion beam **at the pinch exit**. They indicate that the ion fluence range from 7×10^{20} for the lightest gas H_2 decreasing through the heavier gases until a value of 0.8×10^{20} for N_2. For Ne and Ar, the fluence increases to 4.3×10^{20} as radiative collapse constricts the pinch to smaller radius. For Kr and Xe, radiative collapse is even more severe but there is a decrease in fluence down to 0.1×10^{20}. The very small fluence value of Xe is due to the very large energy of the Xe ion, estimated to have average charge state Z_{eff} of 13.6 and accelerated by exceedingly large electric fields induced in the radiative collapse. This complex behavior, deviating from the simple dependence on $(MZ_{eff})^{-1/2}$, noted earlier as apparent from looking at Eqs. (3) and (4), reflects the effects of specific heat ratio and more drastically that of radiative cooling and collapse.

The ion number is 86×10^{14} per kJ for H_2, decreases to 4×10^{14} per kJ for Ne and then to 0.06 for Xe. The ion current decreases from 26% of the discharge current for H_2 to 11% for Ar and drops further to 1% for Xe. The beam energy drops slightly from 7.5% of E_0 for H_2 to 4.7% of E_0 for N_2 and then increases slightly for the radiative collapse gases Ne, Ar, Kr, and Xe. The power flow is highest for Xe at 2.4×10^{10} kW decreasing to 0.7×10^{10} kW for Ar and to 0.4×10^{10} kW for the lighter gases. The damage factor is highest for Xe at $120 \times 10^{10}\,\mathrm{W\,m^{-2}\,s^{0.5}}$ dropping to 14×10^{10} for Ne and to $(2–5) \times 10^{10}$ for the lighter gases. The FPS energy rises from 8% E_0 for H_2 to 15% for Ne and drops to 3%–4% for Kr and Xe. The results for Kr and Xe and to a lesser extent for Ar and even smaller extent for Ne are very much affected by the way the radiative collapse is computed whilst those of the other gases from H_2 to N_2 are not affected by radiative collapse; although N_2 is affected by thermodynamic properties due to its highly, but not fully ionized states.[43] Neon, Ar, Kr, and Xe are also affected by this specific heat ratio effect but in these more radiative gases this effect is completely dominated and masked by radiative cooling and collapse.

Considering the data presented in the table it would appear that for many purposes Ar is a good compromise gas delivering large ion fluence and flux over a relatively large operational pressure with good beam energy, current, power, damage factor, and also plasma stream energy.

We need to emphasize that these calculations pertain to ion beams emitted during the pinch. Recently, it has been postulated that the extended current dips observed in high inductance machines (designated as T2) in several gases including Ar and D_2[8,39,44] are well modeled by the inclusion of anomalous resistance terms into the post-pinch phase of the plasma focus. In particular, Behbahani and Aghamir[39,44] have correlated these post-pinch effects to the detection of multiple ion beams postulated to occur after the pinch. We need to point out that the calculations in this paper do not include these post-pinch emitted ion beams. We also need to emphasize that the calculations of this paper pertain to the ion beam at the exit of the pinch. Measurements on and effects of the fast ion beam and fast plasma stream some distance from the pinch will be attenuated by interaction with the medium traversed and also by beam and stream divergence. The practical importance of these attenuation effects demands further study.

ACKNOWLEDGMENTS

This work was carried out partly within the framework of IAEA Research Contract No. 16934 of CRP F1.30.13 (Investigations of Materials under High Repetition and Intense Fusion-relevant Pulses). We acknowledge a reviewer for valuable comments which led to the writing of the last paragraph of this paper.

[1]S. Lee and S. H. Saw, Phys. Plasmas **19**, 112703 (2012).
[2]S. Lee, Radiative dense plasma focus computation package: RADPF, http://www.plasmafocus.net; http://www.intimal.edu.my/school/fas/UFLF/ (archival websites), 2013.
[3]S. Lee, S. H. Saw, and J. Ali, J. Fusion Energy **32**, 42–49 (2013).
[4]F. N. Beg, I. Ross, A. Lorenz, J. F. Worley, A. E. Dangor, and M. G. Haines, J. Appl. Phys. **88**, 3225–3230 (2000).
[5]V. A. Gribkov, A. Banaszak, B. Bienkowska, A. V. Dubrovsky, I. Ivanova-Stanik, L. Jakubowski, L. Karpinski, R. A. Miklaszewski, M. Paduch, M. J. Sadowski, M. Scholz, A. Szydlowski, and K. Tomaszewski, J. Phys. D: Appl. Phys. **40**, 3592–3607 (2007).
[6]V. N. Pimenov, A. V. Dubrovsky, E. V. Demina, V. A. Gribkov, S. V. Latyshev, S. A. Maslyaev, I. P. Sasinovskaya, and M. Scholz, "Innovative powerful pulsed technique, based on a plasma accelerator, for simulation of radiation damage and testing of materials for nuclear systems," © IAEA, published in http://www-pub.iaea.org/MTCD/publications/PDF/P1433_CD/datasets/papers/at_p5-04.pdf, 2013.
[7]S. Lee and A. Serban, IEEE Trans. Plasma Sci. **24**, 1101–1105 (1996).
[8]S. Lee, S. H. Saw, A. E. Abdou, and H. Torreblanca, J. Fusion Energy **30**, 277–282 (2011).
[9]S. Lee and S. H. Saw, Appl. Phys. Lett. **92**, 021503 (2008).
[10]S. Lee and S. H. Saw, J. Fusion Energy **27**, 292–295 (2008).
[11]S. H. Saw, P. C. K. Lee, R. S. Rawat, and S. Lee, IEEE Trans. Plasma Sci. **37**, 1276–1282 (2009).
[12]S. Lee, R. S. Rawat, P. Lee, and S. H. Saw, J. Appl. Phys. **106**, 023309 (2009).
[13]S. H. Saw and S. Lee, Energy and Power Engineering **2**(1), 65–72 (2010).
[14]M. Akel, Sh. Al-Hawat, S. H. Saw, and S. Lee, J. Fusion Energy **29**(3), 223–231 (2010).
[15]M. Akel, S. Lee, and S. H. Saw, IEEE Trans. Plasma Sci. **40**, 3290–3297 (2012).
[16]S. Lee, "Radiation in plasmas," in *Proceedings of Spring College on Plasma Physics, ICTP, Trieste, 1983*, edited by B. McNamara (World Scientific Pub Co, Singapore, 1984), Vol. II, pp. 978–987.
[17]S. Lee, T. Y. Tou, S. P. Moo, M. A. Elissa, A. V. Gholap, K. H. Kwek, S. Mulyodrono, A. J. Smith, Suryadi, W. Usala & M. Zakaullah. Am. J. Phys. **56**, 62 (1988).
[18]T. Y. Tou, S. Lee, and K. H. Kwek, IEEE Trans. Plasma Sci. **17**, 311–315 (1989).
[19]S. P. Moo, C. K. Chakrabarty, and S. Lee, IEEE Trans. Plasma Sci. **19**, 515–519 (1991).
[20]D. E. Potter, Phys. Fluids **14**, 1911 (1971).
[21]A. Serban and S. Lee, Plasma Sources Sci. Technol. **6**, 78 (1997).
[22]M. H. Liu, X. P. Feng, S. V. Springham and S. Lee, IEEE Trans. Plasma Sci. **26**(2), 135–140 (1998).
[23]S. Lee, P. Lee, G. Zhang, X. Feng, V. A. Gribkov, M. Liu, A. Serban, and T. Wong, IEEE Trans. Plasma Sci. **26**, 1119 (1998).
[24]S. Lee, http://ckplee.home.nie.edu.sg/plasmaphysics/ (archival website), 2013 for containing earliest 5-phase version of the code implemented with effect of small disturbance speed and plasma self-absorption.
[25]D. Wong, P. Lee, T. Zhang, A. Patran, T. L. Tan, R. S. Rawat, and S. Lee, Plasma Sources Sci. Technol. **16**, 116 (2007).
[26]V. Siahpoush, M. A. Tafreshi, S. Sobhanian, and S. Khorram, Plasma Phys. Controlled Fusion **47**, 1065 (2005).

[27]L. Soto, P. Silva, J. Moreno, G. Silvester, M. Zambra, C. Pavez, L. Altamirano, H. Bruzzone, M. Barbaglia, Y. Sidelnikov, and W. Kies, Braz. J. Phys. **34**, 1814 (2004).
[28]H. Acuna, F. Castillo, J. Herrera, and A. Postal, in *International Conference on Plasma Science, 3-5 June* (1996), p. 127.
[29]C. Moreno, V. Raspa, L. Sigaut, and R. Vieytes, Appl. Phys. Lett. **89**, 091502 (2006).
[30]S. H. Saw, M. Akel, P. C. K. Lee, S. T. Ong, S. N. Mohamad, F. D. Ismail, N. D. Nawi, K. Devi, R. M. Sabri, A. H. Baijan, J. Ali, and S. Lee, J. Fusion Energy **31**, 411–417 (2012).
[31]S. Lee, S. H. Saw, R. S. Rawat, P. Lee, A. Talebitaher, A. E. Abdou, P. L. Chong, F. Roy, A. Singh, D. Wong, and K. Devi, IEEE Trans. Plasma Sci. **39**, 3196–3202 (2011).
[32]S. Lee, S. H. Saw, L. Soto, S. V. Springham, and S. P. Moo, Plasma Phys. Controlled Fusion **51**, 075006 (2009).
[33]S. Lee, Plasma Phys. Control. Fusion **50**, 105005 (2008).
[34]S. Lee, Appl. Phys. Lett. **95**, 151503 (2009).
[35]S. Lee and S. H. Saw, J. Fusion Energy **31**, 603–610 (2012).
[36]S. Lee, S. H. Saw, P. C. K. Lee, R. S. Rawat, and H. Schmidt, Appl. Phys. Lett. **92**, 111501 (2008).
[37]S. H. Saw, S. Lee, F. Roy, P. L. Chong, V. Vengadeswaran, A. S. M. Sidik, Y. W. Leong, and A. Singh, Rev. Sci. Instrum. **81**, 053505 (2010).
[38]S. Lee, S. H. Saw, R. S. Rawat, P. Lee, R. Verma, A. Talebitaher, S. M. Hassan, A. E. Abdou, M. Ismail, A. Mohamed, H. Torreblanca, Sh. Al Hawat, M. Akel, P. L. Chong, F. Roy, A. Singh, D. Wong, and K. K. Devi, J. Fusion Energy **31**, 198–204 (2012).
[39]R. A. Behbahani and F. M. Aghamir, J. Appl. Phys. **111**(4), 043304–043305 (2012).
[40]S. H. Saw and S. Lee, Int. J. Energy Res. **35**, 81–88 (2011).
[41]S. P. Chow, S. Lee, and B. C. Tan, J. Plasma Phys. **8**, 21–31 (1972).
[42]Sh. Al-Hawat, M. Akel, S. H. Saw, and S. Lee, J. Fusion Energy **31**, 13–20, (2012).
[43]S. Lee, Aust. J. Phys. **36**, 891–896 (1983).
[44]R. A. Behbahani and F. M. Aghamir, Phys. Plasmas **18**, 103302 (2011).